Macromolecular Materials and Engineering

Macromolecular Materials and Engineering Open Access

www.mame-journal.de

RESEARCH ARTICLE OPEN ACCESS

Polyoxazolines with an Imidazole Terminal Group as Thermal Latent Curing Agents for One-Component Epoxy Resins

Ceren Ozsaltik[1,2] | Cuma Ali Uçar[1,2] | Asu Ece Atespare[1,2] | Bekir Dizman[1,2]

[1]Integrated Manufacturing Technologies Research and Application Center & Composite Technologies Center of Excellence, Sabanci University, Istanbul, Turkey | [2]Faculty of Engineering and Natural Sciences, Materials Science and Nano Engineering, Sabanci University, Istanbul, Turkey

Correspondence: Bekir Dizman (bekirdizman@sabanciuniv.edu)

Received: 13 December 2025 | **Accepted:** 15 December 2025

Keywords: imidazole | one-component epoxy resins | polyoxazoline | thermal latent curing agents

ABSTRACT

Poly(2-oxazoline)-imidazole (POZ-Im) polymers were synthesized by one-pot termination of 2-ethyl, 2-propyl-, and 2-phenyl-2-oxazoline homopolymers with imidazole and evaluated as thermal latent curing agents (TLCs) for one-component epoxy resins (OCERs). ^{1}H NMR, FTIR, and MALDI-TOF confirmed successful synthesis of polymers. The polymers were amorphous, exhibiting glass transition temperatures of 43°C (PEOZ-Im), 24°C (PPrOZ-Im), and 91°C (PPhOZ-Im) and showed thermal stability with onset degradation at 364°C–375°C. When incorporated into DGEBA at a fixed 5 phr Im-to-epoxy ratio, their miscibility and curing performance varied with side-chain chemistry. PPhOZ-Im was fully miscible, PPrOZ-Im was partially miscible, and PEOZ-Im formed fine dispersed domains. Dynamic DSC revealed left-limit temperatures of 91.75°C (PEOZ-Im), 94.22°C (PPhOZ-Im), and 103.28°C (PPrOZ-Im). Rheological analysis showed that PPrOZ-Im/DGEBA exhibited the longest gelation time, followed by PEOZ-Im/DGEBA and PPhOZ-Im/DGEBA. Shelf-life estimations based on viscosity doubling times and Arrhenius extrapolation indicated stability of 88 days (PPrOZ-Im/DGEBA), 34 days (PEOZ-Im/DGEBA), and 32 days (PPhOZ-Im/DGEBA) at −20°C. These results demonstrate that POZ-Im polymers provide tunable latency and curing behavior suitable for advanced composite applications.

1 | Introduction

Composite materials are widely used in engineering applications due to their high performance-to-density properties [1]. Among them, polymer matrix composites (PMCs) are the most prevalent owing to their high mechanical strength, low density, and relatively low processing temperatures [2]. Epoxy resins are used as thermoset matrices in PMCs because they form rigid crosslinked networks with excellent mechanical, thermal, and chemical properties along with strong adhesion to various substrates [3]. The most common epoxy resin is diglycidyl ether of bisphenol A (DGEBA), which provides toughness and rigidity [4, 5].

Curing of epoxy resins results in the formation of a crosslinked network through step-growth or chain-growth polymerization, depending on the curing agent [4]. Primary amines and tertiary amines, such as imidazoles, are widely used for this purpose; however, their high reactivity poses limitations for processing. Epoxy systems are formulated either as two-component systems or, increasingly, as one-component epoxy resins (OCERs). Two-component epoxy systems must be mixed immediately before use and suffer from short pot life and mixing sensitivity, which hinder large-scale manufacturing and process control, raising production and storage costs [6]. In contrast, OCERs offer extended shelf life, improved reproducibility, minimized processing errors, and suitability for automated and large-scale manufacturing, leading

to cost and energy savings [7]. This functionality is enabled by latent curing agents that remain inactive at ambient conditions and activate only under external stimuli such as radiation or heat [4].

The performance and storage stability of OCERs are therefore strongly dependent on the design of effective latent curing agents. Among latent curing agents, thermal latent curing agents (TLCs) are the most common. TLCs function either through limited solubility of the active species (e.g., crystalline agents or encapsulated catalysts) or via precursors that undergo structural activation upon heating [4]. Dicyandiamide (DICY) is one of the most common crystalline TLCs; its latency arises from low solubility in epoxy resin at room temperature. Curing begins upon melting at around 170°C, providing excellent mechanical performance and storage stability, but at the cost of a high curing temperature and a slow rate, often necessitating the use of accelerators [8, 9]. Other systems, such as aminopyridine-based dual-locked TLCs, utilize chemical deactivation mechanisms to suppress reactivity at room temperature and tune curing onset between 120°C–150°C [10]. Although imidazoles offer high heat resistance and catalytic efficiency, their room-temperature reactivity prevents their direct use in OCERs. Efforts to develop stable imidazole derivatives with sufficient latency have had limited success [7, 11], prompting interest in polymer-supported systems.

Polymer-based TLCs have emerged as a promising approach to overcome the limitations of conventional systems by combining long shelf life with controlled activation and energy-efficient curing. Two main strategies are used: physical encapsulation and covalent bonding of curing agents within a polymer matrix. In the encapsulation approach, active curing agents such as imidazoles are entrapped in polymers like polyethylene glycol (PEG), polycaprolactone (PCL), polystyrene (PS), poly(methyl methacrylate) (PMMA), poly(vinyl acetate) (PVAc), or poly(ether imide) (PEI) via solvent evaporation, emulsification, or spray-drying techniques [8, 12–15]. The polymer structure and polarity significantly affect the latency and curing behavior. Recently, poly(2-oxazoline)s (POZs) have drawn attention as alternative matrices due to their tunable structures and ability to form hydrogen-bonded complexes with imidazoles. These complexes inhibit the catalytic activity of imidazole at room temperature but dissociate upon heating, restoring reactivity [16–18]. Covalent bonding offers stronger latency, where curing agents and catalysts are immobilized until thermal activation occurs. For instance, PEG–Im polymers enhance latency and shelf life, and polymeric imidazole accelerators synthesized through copolymerization offer temperature-dependent solubility, preventing premature curing [11, 19, 20]. However, such systems often require multistep syntheses and lack precise structural control, motivating further development.

Poly(2-oxazoline)s (POZs) are a versatile class of polymers first reported in 1966 and have since gained prominence, particularly in biomedical applications, due to their nonionic, biocompatible, and chemically stable nature [21–24]. Structurally, POZs resemble polypeptides, containing tertiary amide bonds along the backbone that confer high stability [25]. They are synthesized via living cationic ring-opening polymerization (CROP) of 2-oxazoline monomers, which allows precise control over molecular weight, end-group functionality, and side-chain composition. By tuning side-chain length and polarity, POZs can exhibit a wide range of solubilities and thermal stabilities. Poly(2-methyl-2-oxazoline) is highly hydrophilic, whereas longer alkyl or aromatic substituents reduce water solubility and increase hydrophobicity [26, 27]. Their thermal stability extends up to 300°C, and the glass transition temperature (T_g) decreases with increasing side-chain length, while crystallinity appears for longer alkyl substituents [28].

While previously reported POZ/imidazole latent curing systems rely exclusively on physical entrapment of imidazole, there are no existing studies that incorporate covalent bonding within POZ-based systems. The present work introduces covalently bonded POZ-imidazole (POZ-Im) structures to achieve enhanced stability and more predictable latency.

In this study, polymer-based TLCs were developed using POZs to stabilize imidazole and fine-tune the curing temperature of OCERs. Homopolymers of 2-ethyl-, 2-propyl-, and 2-phenyl-2-oxazoline with a target molecular weight of 1,000 g/mol were synthesized and terminated with imidazole to obtain covalently bonded POZ-Im polymers. The chemical structure, molecular weight, and dispersity of the polymers were characterized by ^{1}H NMR, FTIR, and MALDI-TOF. Thermal properties such as T_g, crystallinity, and degradation were analyzed by DSC and TGA to evaluate the influence of side-chain structure. The POZ-Im polymers were then employed as TLCs in DGEBA-based OCERs. The effect of POZ hydrophilicity on curing behavior was investigated using DSC, focusing on left limit and peak temperatures, enthalpy, and conversion. Gelation behavior was studied rheologically, and storage stability was assessed through accelerated aging tests to estimate shelf life at low temperatures. The study aims to demonstrate that controlled polymer architectures can enhance imidazole latency and provide tunable curing characteristics for energy-efficient, process-stable epoxy systems suitable for advanced adhesive and composite applications.

2 | Experimental

2.1 | Materials

2-Ethyl-2-oxazoline (EOZ) (≥99%), 2-phenyl-2-oxazoline (PhOZ) (99%), chlorobenzene (99%), bisphenol A diglycidyl ether (DGEBA, molar mass: 340.41 g·mol^{-1}), and imidazole (≥ 99%) were purchased from Sigma-Aldrich. Monomers and chlorobenzene were dried over calcium hydride (CaH_2), distilled, and kept over 4Å molecular sieves before their use in polymerizations. Trifluoromethanesulfonic acid (TfOH) (99%) was purchased from Acros Organics. Butyronitrile (99%) was purchased from ABCR. Ethanolamine (≥99%), CaH_2 (97%), dichloromethane (DCM) (≥99.9%), zinc acetate dihydrate ($Zn(OAc)_2{\cdot}2H_2O$) (≥99.5%), and sodium sulfate (Na_2SO_4) (≥99%) were purchased from Merck. Deionized water was acquired from Merck Direct-Q-3 UV. Unless it is stated otherwise, all chemicals were used as received.

2.2 | Instruments

$CDCl_3$ was used as a solvent for recording ^{1}H NMR spectra on a 60 MHz Varian spectrometer. FTIR spectra were obtained

on a ThermoScientific Nicolet iS50 FTIR spectrometer using an attenuated total reflectance (ATR) accessory. The transmission mode was used, and the resolution was 4 cm^{-1}. DSC measurements were carried out using a Mettler Toledo DSC 3+ instrument. DSC thermograms were obtained from the second heating run at 10°C/min from 25°C to 300°C, after the first run of heating up to 200°C and cooling down to −50°C at 10°C/min, under a nitrogen atmosphere, to measure the glass transition temperatures (T_g). TGA measurements were performed on a Mettler Toledo TGA/DSC 3+ in the range of 25°C to 800°C. Samples of 10–100 mg were heated at 10°C/min under a nitrogen atmosphere with a flow rate of 100 mL/min. Conditioning at 110°C for 30 min was performed on samples prior to analysis. Molecular weights were measured with MALDI TOF (Bruker microflex LT MALDI TOF MS) using α-cyano-4-hydroxycinnamic acid and sodium iodide.

The dispersion quality of the TLCs in the DGEBA resin was examined with a Nikon Eclipse LV100ND optical microscope equipped with CFI60–2 lenses at magnifications of 25x, 50x, 100x, and 200x. Bright-field illumination was applied from beneath the material during imaging. Curing studies were performed on a Mettler Toledo HP DSC 2+ instrument. The samples were weighed in amounts of 10–15 mg on the DSC pans. The dynamic DSC thermograms were obtained from the first heating run in the range of 25°C to 250°C with a heating rate of 10°C/min under a nitrogen atmosphere. Isothermal DSC measurements were performed for 3 h at various temperatures, followed by dynamic DSC tests from 25°C to 250°C at a heating rate of 10°C/min to measure the residual enthalpy. Temperature and time sweep rheology analyses were performed with an Anton-Paar MCR 302 Rheometer using a gap of 0.5 mm, a shear strain of 1%, and a frequency of 10 rad/s.

2.3 | Synthesis of Monomers and POZ-IM Polymers

2.3.1 | Synthesis of Monomers

2.3.1.1 | Preparation of 2-Ethyl-2-Oxazoline (EOZ) and 2-Phenyl-2-Oxazoline (PhOZ). EOZ and PhOZ were commercially available. Trace amounts of water and impurities in the monomers were removed by distillation before the polymerization reactions. The monomers were dried over calcium hydride (CaH_2) overnight and then purified by distillation under N_2 flow. The purified colorless liquid monomers were stored with 4A° molecular sieves.

2.3.1.2 | Synthesis of 2-Propyl-2-Oxazoline (PrOZ). PrOZ was synthesized using the nitrile route in the literature [29]. Butyronitrile (60 g, 0.87 mol, 1 eq.), ethanolamine (58.5 g, 0.95 mol, 1.1 eq.), and a catalytic amount of $Zn(OAc)_2.2H_2O$ (3.82 g, 0.017 mol, 0.02 eq.) were mixed in a 250 mL flask. The reaction mixture was heated to 130°C and kept under reflux for 16 h. After adding 200 mL of DCM to the mixture, the organic phase was washed twice with DI water and once with brine solution. The organic phase was separated and dried over Na_2SO_4. After the drying step, sodium sulfate was filtered. DCM present in the filtrate was evaporated under reduced pressure. After distillation, a colorless liquid monomer was obtained (52 g, yield: 53%). The synthesized monomer was stored on 4A° molecular sieves.

2.3.2 | General Synthesis Procedure of POZ-Im Polymers

Polymerizations were conducted in two-necked round-bottom flasks, dried at 120°C, and cooled under nitrogen purge. A 4 M concentration of monomers in chlorobenzene was used for the polymerizations, considering the total concentration of monomers in each reaction. TfOH was used as the initiator, and termination was done with imidazole dissolved in DCM overnight (Figure 1).

To obtain polymers with a molar mass of 1000 g/mol, a monomer-to-initiator ratio ([M]/[I]) of 10 was used. Table 1 summarizes the reaction conditions for polymerization.

2.3.2.1 | Synthesis and Purification of PEOZ-Im. To synthesize the PEOZ-Im, EOZ (33 g, 0.33 mol), chlorobenzene (83 mL), and TfOH (2.945 mL, 0.033 mol, [M]/[I] = 10) were added to a 250 mL round-bottom flask, and the polymerization solution was mixed while being purged with N_2. The flask was immersed in a pre-heated oil bath to heat the reaction mixture to 80°C. After 30 min, the flask was placed in an ice bath. For the termination process, imidazole (4.53 g, 0.066 mol, 2 eq) dissolved in DCM (80 mL) was added to the reaction mixture at room temperature and stirred overnight.

After the termination process was completed, the solvents were removed by rotary evaporator. The resulting solid residue was first dissolved in an acidic brine solution and extracted with DCM. The organic phase was collected, and DCM was evaporated with a rotary evaporator. Second, it was dissolved in a basic brine solution and extracted with DCM. After these processes, the organic phase was dried with Na_2SO_4. The filtration of the mixture was followed by the evaporation of the filtrate at room temperature under reduced pressure, and the polymer was recovered from methanol as a white fluffy solid (yield: 81 %).

2.3.2.2 | Synthesis and Purification of PPrOZ-Im. To synthesize the PPrOZ-Im, PrOZ (40 g, 0.35 mol), chlorobenzene (88 mL), and TfOH (2.843 mL, 0.035 mmol, [M]/[I] = 10) were added to a 250 mL round-bottom flask, and the polymerization solution was mixed while being purged with N_2. The flask was immersed in a pre-heated oil bath to heat the reaction mixture to 80°C. After 30 min, the flask was placed in an ice bath. For the termination process, imidazole (4.37 g, 0.07 mol, 2 eq) dissolved in DCM (80 mL) was added to the reaction mixture at room temperature and stirred overnight.

After the termination process was completed, the solvents were removed by rotary evaporator. The resulting solid residue was dissolved in DCM and washed with DI water. After the organic phase was dried with Na_2SO_4 and filtered, DCM was removed under reduced pressure. The polymer was recovered from methanol as a white fluffy solid (yield: 84 %).

2.3.2.3 | Synthesis and Purification of PPhOZ-Im. To synthesize the PPhOZ-Im, PhOZ (49 g, 0.33 mol), chlorobenzene (83 mL), and TfOH (2.946 mL, 0.033 mmol, [M]/[I] = 10) were

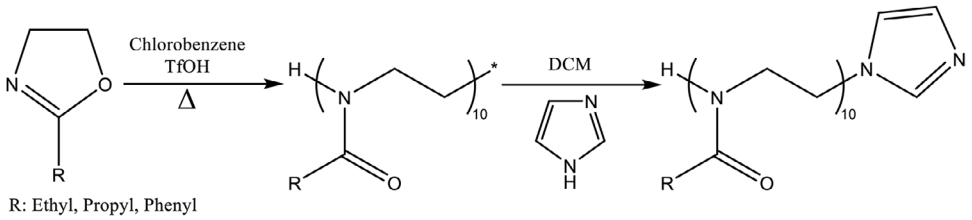

FIGURE 1 | Synthesis of POZs with an imidazole terminal group.

TABLE 1 | Polymerization conditions.

POZ-Im	Polymerization Temperature (°C)	Polymerization Time (min)
PEOZ-Im	80	30
PPrOZ-Im	80	30
PPhOZ-Im	95	60

added to a 250 mL round-bottom flask, and the polymerization solution was mixed while being purged with N_2. The flask was immersed in a pre-heated oil bath to heat the reaction mixture to 95°C. After 60 min, the flask was placed in an ice bath. For the termination process, imidazole (4.53 g, 0.066 mol 2 eq) dissolved in DCM (80 mL) was added to the reaction mixture at room temperature and stirred overnight.

After the termination process was completed, chlorobenzene and DCM were removed by rotary evaporator. The resulting solid residue was dissolved in DCM and washed with DI water. After the organic phase was dried with Na_2SO_4 and filtered, DCM was removed under reduced pressure. The remaining polymer was dissolved in methanol and precipitated in cold diethyl ether (MeOH: DEE = 1:10). After precipitation, the polymer was filtered and dried in a desiccator (yield: 80 %).

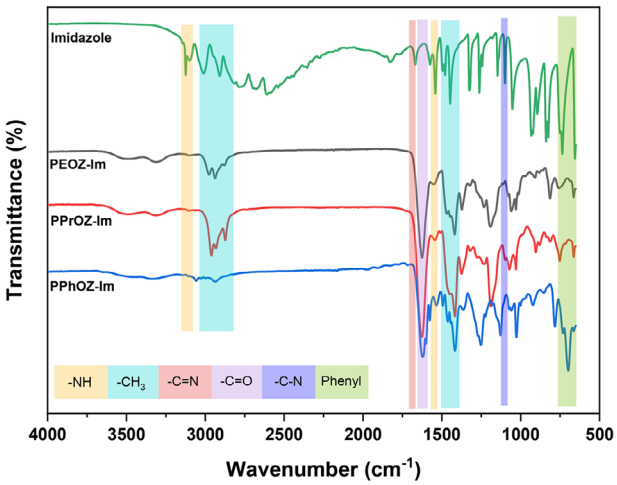

FIGURE 2 | FTIR spectra of PEOZ-Im, PPrOZ-Im, PPhOZ-Im, and pure imidazole.

2.4 | Preparation of the OCERs

The prepared POZ-Im polymers were cooled to subzero temperature with liquid nitrogen and then ground with a mortar and pestle. The ground powder was mixed with DGEBA resin at 5% molar ratio (imidazole to epoxy ratio) using a homogenizer in a glass vial at 1500 rpm for 15 min. The sample was degassed, sealed with a cap, covered with parafilm, and stored in a fridge at −18°C.

3 | Results and Discussion

3.1 | Structural Analysis of Synthesized POZ-IM Polymers

FTIR and ^{1}H NMR analyses were performed for the structural characterization of the synthesized polymers. The FTIR spectra presented in Figure 2 suggest the effective removal of free imidazole as indicated by the disappearance of the -NH stretching and bending vibrations at 3125 and 1540 cm^{-1} belonging to imidazole. The broad peak observed at 3500 cm^{-1} corresponds to the hydroxyl group of water absorbed by the polymers. The peaks between 2900–3000 cm^{-1} belong to the CH_3 and CH_2 stretching vibrations, while the peak observed at 1620 cm^{-1} is associated with the carbonyl group of the POZ amide groups. In addition, the characteristic imidazole ring vibrations at 1098 and 1261 cm^{-1} indicate that imidazole is present within the polymer backbone, but not in its free form. The sharp C═N stretching peak is observed at 1668 cm^{-1} in the imidazole spectrum, while in the POZ-Im spectra, this peak overlaps with the broad C═O stretching band, making it indistinguishable as a separate signal. The peak at 700 cm^{-1} is associated with the phenyl out-of-plane bending vibration, which confirms the presence of the phenyl structure. These results align well with the expected polymer structures.

^{1}H NMR spectra of imidazole, PEOZ-Im, and their physical mixture were compared to confirm that the imidazole-related peaks do not belong to the free imidazole but come from covalently bonded imidazole (Figure 3a). The NH proton (C) appears at 12 ppm while the aromatic protons (A and B) are observed at 7.69 and 7.10 ppm. While they are physically mixed, these peaks shifted and new peaks arose between 7.00–7.50 ppm, which are associated with covalently bonded imidazole (a, b,

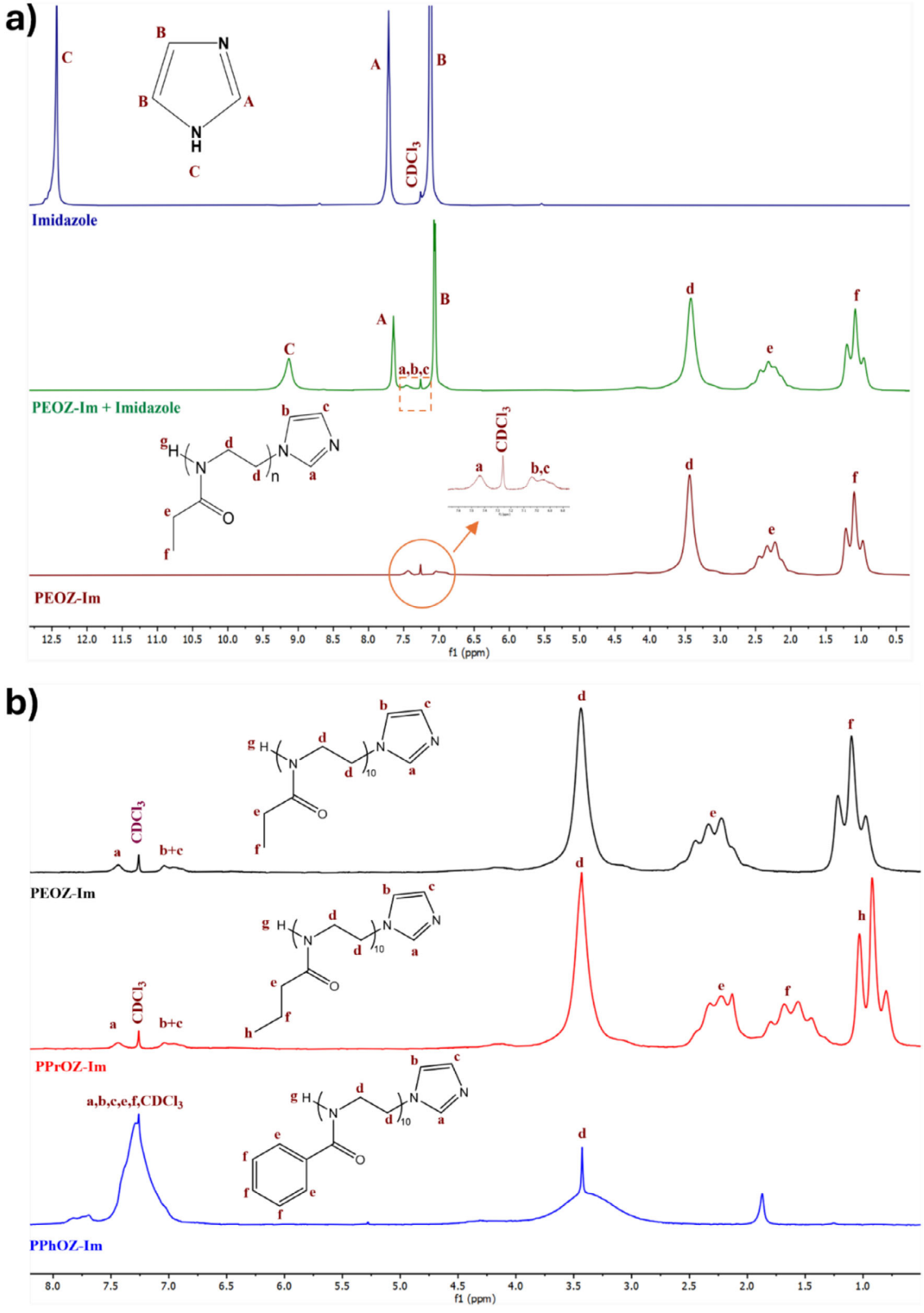

FIGURE 3 | ^{1}H NMR spectra of (a) imidazole, its physical mixture with PEOZ-Im, and covalently bonded PEOZ-Im; (b) PEOZ-Im, PPrOZ-Im, and PPhOZ-Im.

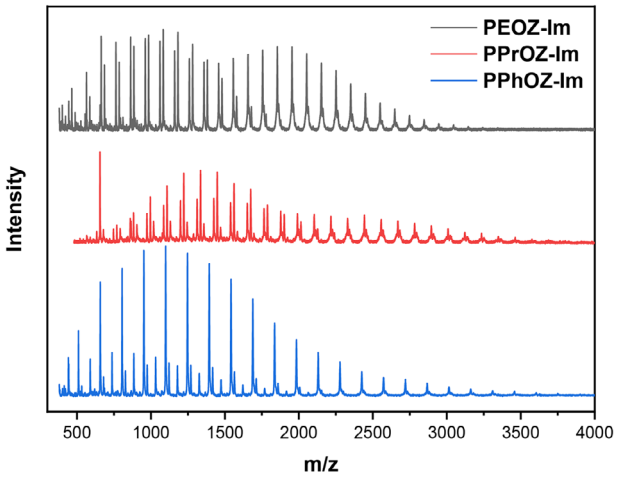

FIGURE 4 | MALDI-TOF analysis results of the synthesized POZ-Im polymers.

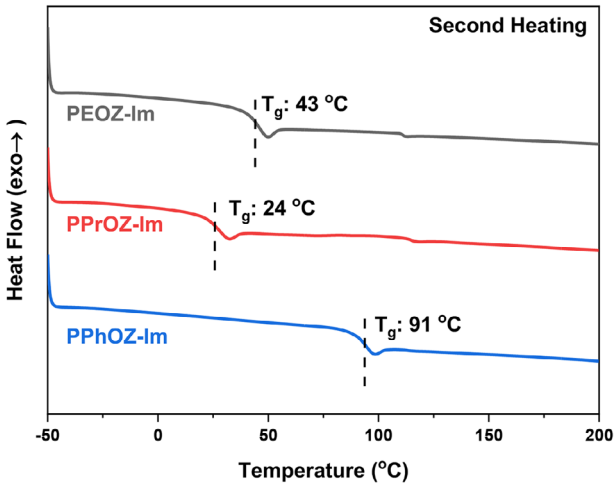

FIGURE 5 | DSC thermograms of POZ-Im polymers.

TABLE 2 | Molecular weight results of POZ-Im polymers.

Polymer-Im	M_n (g/mol)	M_w (g/mol)	PDI
PEOZ-Im	1470	1760	1.20
PPrOZ-Im	1600	1870	1.17
PPhOZ-Im	1340	1640	1.23

and c). The significant shift in the NH peak was attributed to the hydrogen bonding between the free imidazole and the polymer. Additionally, the absence of free imidazole peaks in the purified PEOZ-Im spectrum confirms that the peaks between 7.00–7.50 ppm belong to covalently bonded imidazole, and free imidazole has been successfully removed.

The ^{1}H NMR spectra of PEOZ-Im, PPrOZ-Im, and PPhOZ-Im given in Figure 3b confirm the successful synthesis, termination, and purification of all the POZ-Im polymers. Broad peak shapes are consistent with a polymeric structure. The characteristic covalently bonded imidazole peaks were observed in all spectra, appearing between 7.00–7.50 ppm (a, b, and c). The polymer backbone and side-chain signals are observed in their expected regions. The peaks corresponding to the methyl protons of the side chain groups of the polymers appear at 1.1 ppm (f) for PEOZ and 0.96 ppm for PPrOZ (h). The backbone peak is observed at 3.42 ppm (d). For PPhOZ-Im, aromatic protons from the phenyl side groups appeared between 6.8–7.4 ppm (e and f), overlapping with the imidazole signals. The amide NH proton (g) was not distinctly visible, likely due to exchange broadening in $CDCl_3$ in the presence of polymer and a trace of moisture, which comes with the polymer. Also, the NMR data align well with the expected polymer structures, confirming the successful progression of the reaction.

The molecular weight and polydispersity (PDI) values of the synthesized POZ-Im polymers measured by MALDI-TOF using α-cyano-4-hydroxycinnamic acid and sodium iodide are presented in Figure 4 and Table 2. All three samples showed sharp and evenly spaced peaks, confirming the successful polymerization. The spacings between peaks in each spectrum corresponded well with the theoretical molecular weight of the repeat units (99.13 Da for 2-ethyl-2-oxazoline, 113.16 Da for 2-propyl-2-oxazoline, and 147.17 Da for 2-phenyl-2-oxazoline). The m/z values of the peaks confirm the presence of the imidazole end group and sodium adduct. The molecular weight values are slightly higher than the targeted value (1000 g/mol), which may be attributed to the presence of moisture in the reaction environment. The relatively narrow PDI values (1.20, 1.17, and 1.23) indicate a controlled polymerization process, resulting in polymers with uniform molecular weight distributions.

3.2 | Thermal Properties of Synthesized POZ-Im Polymers

Thermal properties of the POZ-Im polymers were investigated by DSC and TGA. The effect of polymer side groups on thermal properties was investigated by DSC. The second heating thermograms of the DSC analysis are provided in Figure 5. All polymers lacked melting or crystallization peaks and exhibited amorphous behavior. The glass transition temperatures (T_gs) of PEOZ-Im, PPrOZ-Im, and PPhOZ-Im polymers were 43°C, 24°C, and 91°C, respectively. The lower T_g of PPrOZ-Im compared to PEOZ-Im can be explained by the longer propyl side chains, which reduce the chain stacking density, provide more free space, and enhance chain mobility. The significantly higher T_g of PPhOZ-Im than the T_g values of aliphatic chain polymers is due to the π-stacking of rigid aromatic phenyl side chains, which hinder chain mobility through stronger interchain interactions.

TGA and DTGA analyses were performed to investigate the thermal stability and degradation behavior of the polymers (Figure 6). All polymers exhibited high thermal stability, with $T_{d5\%}$ values of 352°C (PEOZ-Im), 366°C (PPrOZ-Im), and 358°C (PPhOZ-Im). The onset degradation temperatures (T_d) determined by the tangent method were 364°C, 387°C, and 375°C for PEOZ-Im, PPrOZ-Im, and PPhOZ-Im, respectively. These values confirm that the introduction of imidazole end groups does not compromise the high thermal robustness of POZ backbones.

The DTGA curves (Figure 6b) provide further insight into the degradation mechanism. The main DTGA peaks are located at

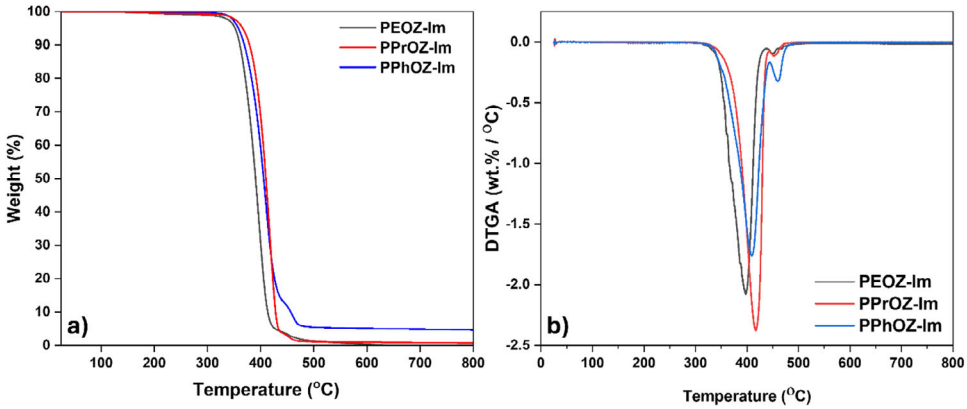

FIGURE 6 | (a) TGA and (b) DTGA thermograms of POZ-Im polymers.

398°C for PEOZ-Im, 417°C for PPrOZ-Im, and 410°C for PPhOZ-Im, in agreement with the relative onset temperatures and demonstrating that PPrOz-Im decomposes at higher temperatures. In all three polymers, a dominant single degradation step is observed, accompanied only by very small secondary peaks at higher temperatures (450°C, 453°C, and 460°C for PEOZ-Im, PPrOZ-Im, and PPhOZ-Im, respectively). These minor high-temperature features likely correspond to the final breakdown of the residual fragments or slow oxidation of char and do not represent a separate major decomposition process. For PPhOZ-Im, the presence of aromatic side groups slightly broadens the main DTGA peak and intensifies the high-temperature shoulder, consistent with the additional stability of phenyl substituents.

Across all samples, thermal decomposition was nearly complete, with less than 5% residue, indicating the effectiveness of the purification processes. Overall, the TGA/DTGA results show that all POZ-Im polymers possess high thermal stability, with degradation temperatures well above their curing and application windows.

3.3 | Compatibility of POZ-Im Polymers With DGEBA

Since POZ-Im polymers in epoxy resins are targeted to be used for composite applications, understanding the compatibility of the POZ-Im with epoxy resin, the curing behavior of the OCERs formulated with epoxy resin and POZ-Im, and the rheological properties of these OCERs are critical. In this study, DGEBA resin was used. To gain insight into the behavior of these systems, samples were prepared using POZ-Im/DGEBA mixtures with an imidazole-to-epoxy molar ratio of 5%. The morphology of the mixtures was investigated with an optical microscope before the curing process. Dynamic and isothermal DSC analyses were then performed to investigate curing behavior.

Optical microscope images of POZ-Im/DGEBA OCERs are shown in Figure 7. Following 20 min of homogenization, the PEOZ-Im/DGEBA OCER exhibits a fine, uniform dispersion characterized by numerous tiny particles. This results from poor compatibility and limited miscibility of PEOZ in DGEBA related to their differing hydrophilicity, with PEOZ being more hydrophilic than DGEBA. Conversely, PPrOZ-Im/DGEBA and PPhOZ-Im/DGEBA OCERs exhibit a clear background apart from the air bubbles, suggesting good miscibility. Due to the higher hydrophobicity of propyl side chains compared to ethyl groups, PPrOZ-Im exhibits enhanced compatibility with DGEBA relative to PEOZ-Im. PPhOZ-Im, the most hydrophobic of the three polymers, exhibits a very good compatibility with DGEBA, attributed to the π–π stacking of aromatic phenyl groups with DGEBA.

3.4 | Curing behavior of POZ-Im/DGEBA OCERs

Dynamic DSC thermograms of the POZ-Im/DGEBA OCERs are presented in Figure 8. All samples showed a low-temperature shoulder around 110–125°C followed by a main exothermic peak in the thermograms, indicating a 2-step curing mechanism.

This feature represents an early activation step typical of imidazole-initiated epoxy systems. As reported in the literature, differential scanning calorimetry often shows two exothermic events in imidazole-catalyzed curing: an initial low-enthalpy process associated with imidazole regeneration via β-elimination or N-dealkylation, followed by the main anionic ring-opening polymerization of epoxy groups with the regenerated imidazole [4]. The small shoulder observed here corresponds to the onset of catalytic activity rather than a distinct reaction mechanism, and the primary curing reaction is represented by the dominant exothermic peak at higher temperature. The absence of a secondary gelation process rheologically confirms that no separate curing mechanism is occurring.

Following activation, a strong main exotherm corresponding to rapid network formation was observed. The left limit temperatures of the samples containing PEOZ-Im, PPrOZ-Im, and PPhOZ-Im were determined as 91.75°C, 103.28°C, and 94.22°C, respectively, while the corresponding peak temperatures were 153°C, 167°C, and 163°C. In addition, the curing enthalpies (ΔH) were measured as 151.26, 86.12, and 89.11 J/g. These results suggest that the polymer side chain structure and the resulting morphology in the epoxy matrix influence both the curing kinetics and thermal reactivity.

Among the samples, PEOZ-Im exhibited the highest curing enthalpy, implying a higher degree of crosslinking or more

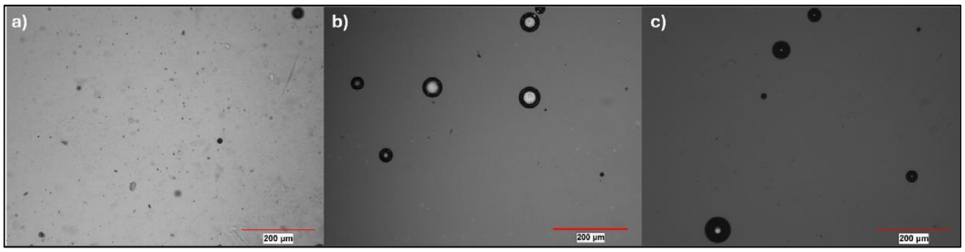

FIGURE 7 | Optical images of OCERs at 100x (a) PEOZ-Im/DGEBA, (b) PPrOZ-Im/DGEBA, (c) PPhOZ-Im/DGEBA.

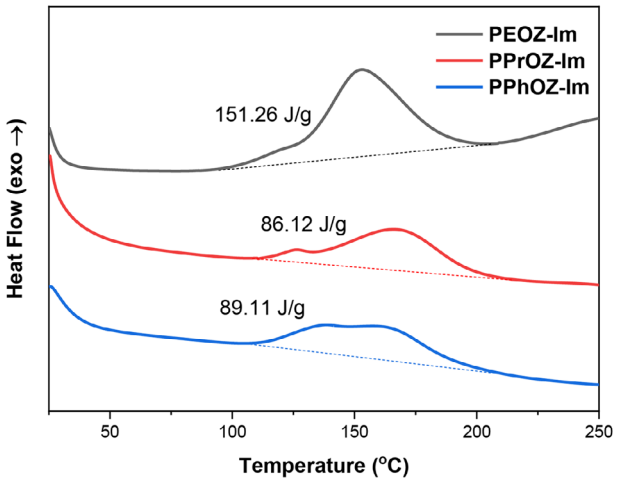

FIGURE 8 | Dynamic DSC thermograms of POZ-Im/DGEBA OCERs.

complete curing compared to the others. Also, it displayed the earliest left limit temperature, suggesting a rapid curing process, probably because of early reaction due to local accumulation of imidazole. In contrast, PPrOZ-Im and PPhOZ-Im exhibited lower enthalpies, indicating a slower or less complete curing reaction under identical conditions, probably due to the steric hindrance of bulkier side chains than ethyl. Although both PPrOZ-Im and PPhOZ-Im exhibited good compatibility with DGEBA, the more delayed curing behavior of PPrOZ-Im can be explained not by solubility but by the effect of side chains. The flexible nature of the propyl side chains may lead to more coiled conformations, separating imidazole groups from the epoxy network, and hindering interaction between imidazole and epoxy groups at low temperatures. In contrast, PPhOZ-Im has rigid, planar groups, which may not sterically hinder imidazole as effectively, and may facilitate closer alignment of imidazole and stronger interactions with DGEBA through π–π stacking, thereby facilitating earlier activation and curing despite exhibiting comparable macroscopic dispersion behavior.

Compared to free imidazole, which typically initiates curing at lower temperatures, covalently bonded POZ-Im polymers exhibit enhanced latency and more controlled activation profiles. The absence of exothermic activity below 90°C in all DSC thermograms further supports the thermal latency of POZ-Im-based curing systems, ensuring storage stability at ambient conditions, demonstrating their potential as effective TLCs.

To further evaluate the curing behavior of the POZ-Im based OCERs, isothermal DSC tests were performed at temperatures of 60°C, 80°C, 100°C, 120°C, and 140°C for 3 h to as shown in Figure 9. Following the isothermal DSC step, dynamic scans were carried out between 25°C and 250°C at a heating rate of 10°C /min to determine the residual enthalpy. The total enthalpy values (isothermal + dynamic) were higher than those obtained from the dynamic test alone (Figure 8), indicating enhanced curing due to the longer reaction time provided under isothermal conditions, allowing more curing. The total conversion at each isothermal step was calculated based on the ratio of isothermal to total enthalpy, as summarized in Table 3. Across all systems, increasing the isothermal test temperature resulted in higher isothermal curing enthalpies and lower residual enthalpies, confirming that cure advancement is strongly temperature dependent. This trend supports the effective thermal latency of the POZ-Im TLCs at low temperatures and their efficient activation at elevated temperatures.

The isothermal DSC data in Table 3 reveal clear differences in curing kinetics among the three POZ-Im systems. Minimal curing occurred at 60°C for PEOZ-Im/DGEBA (4.74%), while almost no significant curing was observed for PPrOZ-Im/DGEBA and PPhOZ-Im/DGEBA OCERs at the same temperature. Also, at 80°C, PEOZ-Im/DGEBA OCER reached 74.6% conversion while PPrOZ-Im/DGEBA and PPhOZ-Im/DGEBA OCERs achieved only 59.4% and 55.3% respectively. These results indicate that while all systems remain latent at low temperatures, PEOZ-Im begins to activate earlier. The earlier activation of PEOZ-Im is consistent with its partially phase-separated morphology, where finely dispersed domains facilitate earlier catalytic accessibility. In contrast, the homogeneous morphology of PPhOZ-Im promotes rapid curing once activation begins but still delays initiation at low temperatures due to stronger PPhOZ-Im interactions.

At higher temperatures, the distinct curing profiles become more pronounced. Both PEOZ-Im/DGEBA and PPhOZ-Im/DGEBA OCERs reached complete curing at 120°C; PPrOZ-Im/DGEBA OCER required a higher temperature of 140°C to reach 100% conversion. This behavior is consistent with rheological results, where PPrOZ-Im/DGEBA OCER exhibits the longest gelation time and dynamic DSC left limit, confirming it has the highest thermal latency of the three OCERs. PPhOZ-Im/DGEBA cures the fastest once activated, likely due to its higher miscibility and more accessible catalytic environment. PEOZ-Im/DGEBA displays intermediate behavior, activating slightly earlier than PPhOZ-Im/DGEBA but showing a balanced combination of latency and reactivity.

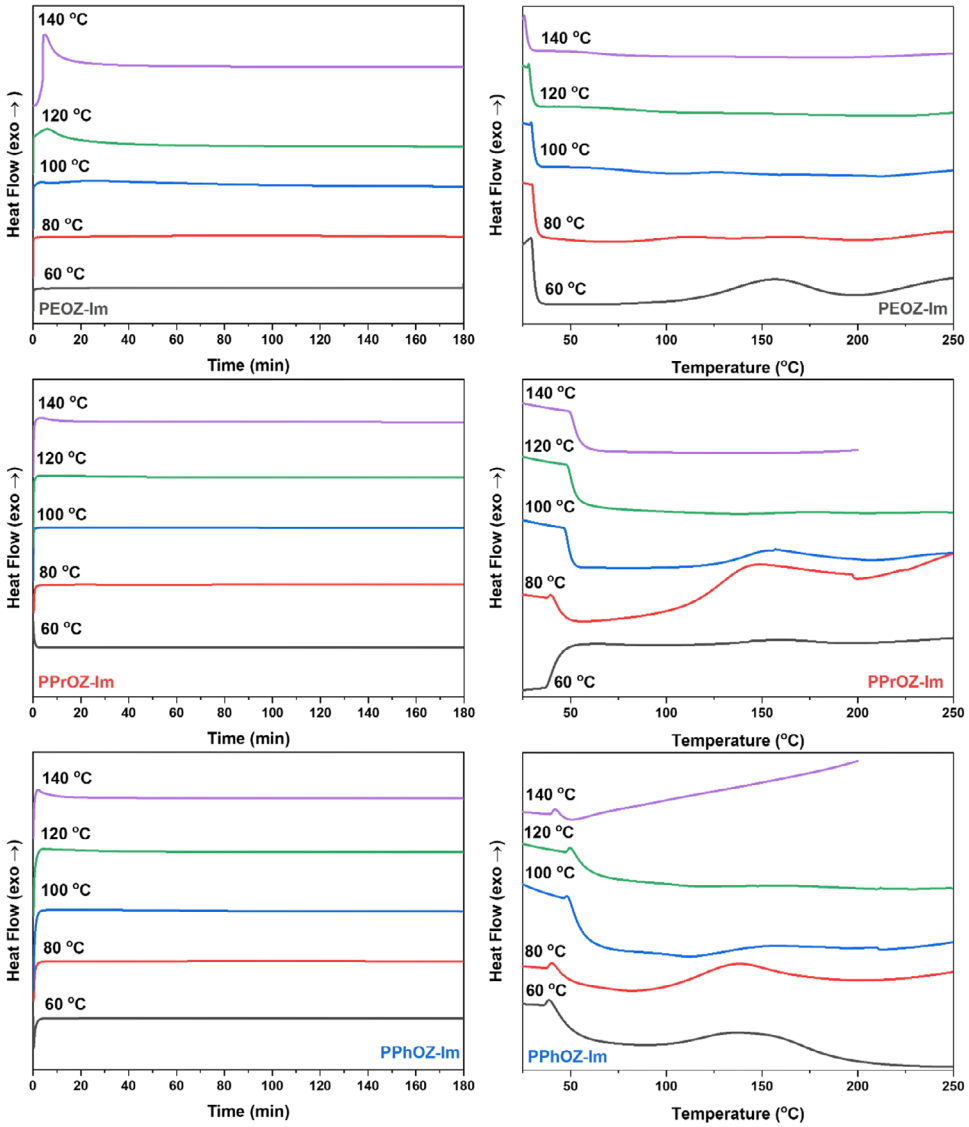

FIGURE 9 | Isothermal DSC and following dynamic DSC thermograms of POZ-Im/DGEBA OCERs.

The steep increase in isothermal enthalpy between 80°C and 100°C for all systems suggests a transition from diffusion-limited to chemically controlled curing, typical of imidazole-catalyzed anionic ring-opening polymerization. The sharper transition observed for PPhOZ-Im/DGEBA indicates faster catalytic turnover once the activation barrier is surpassed.

Overall, the isothermal DSC results confirm that the curing behavior of POZ-Im polymers is strongly influenced by side-chain structure, enabling tunable latency and activation temperatures for targeted OCER applications.

3.5 | Stability of POZ-Im/DGEBA OCERs

Following the DSC analysis of thermal latency, viscosity, storage modulus (G'), and loss modulus (G″) of the mixtures were evaluated through temperature sweep and isothermal measurements within their linear viscoelastic region. This allowed for the determination of gelation temperatures and shelf lives of the mixtures.

Gelation temperatures are determined by the crossover point of storage modulus and loss modulus. According to the temperature sweep provided in Figure 10, the gelation temperatures of the PEOZ-Im/DGEBA, PPrOZ-Im/DGEBA, and PPhOZ-Im/DGEBA OCERs were found as 123°C, 138°C, and 128°C, respectively. These values align well and support the findings obtained from DSC analyses, providing evidence that gelation (network formation) occurs after the latent period identified in DSC and suggests the temperature-dependent activation of the imidazole groups.

The more delayed gelation observed for PPrOZ-Im/DGEBA OCER is consistent with a higher curing left limit and peak temperatures in DSC. In contrast, PEOZ-Im/DGEBA and PPhOZ-Im/DGEBA OCERs gelled at a lower temperature, suggesting earlier curing initiation. Additionally, PEOZ-Im-based OCER exhibited the fastest rise in viscosity and G', indicating rapid network formation upon curing initiation.

In the isothermal rheology scans (Figure 11), the time required for the initial viscosity to double was defined as the shelf life.

TABLE 3 | Isothermal DSC results of POZ-Im/DGEBA OCERs.

POZ-Im (TLC)	Isothermal Temperature (°C)	Normalized Isothermal Enthalpy (J/g)	Residual Enthalpy (J/g)	Conversion at Isothermal Temperature (%)
PEOZ-Im	60	4.08	81.94	4.74
	80	86.26	29.37	74.60
	100	98.26	4.22	95.88
	120	179.28	—	100
	140	267.71	—	100
PPrOZ-Im	60	—	210.35	0
	80	157.23	107.51	59.39
	100	162.16	37.71	81.13
	120	246.84	2.73	98.91
	140	213.72	—	100
PPhOZ-Im	60	—	69.01	0
	80	78.20	63.12	55.34
	100	230.22	14.93	93.91
	120	173.25	—	100
	140	193.29	—	100

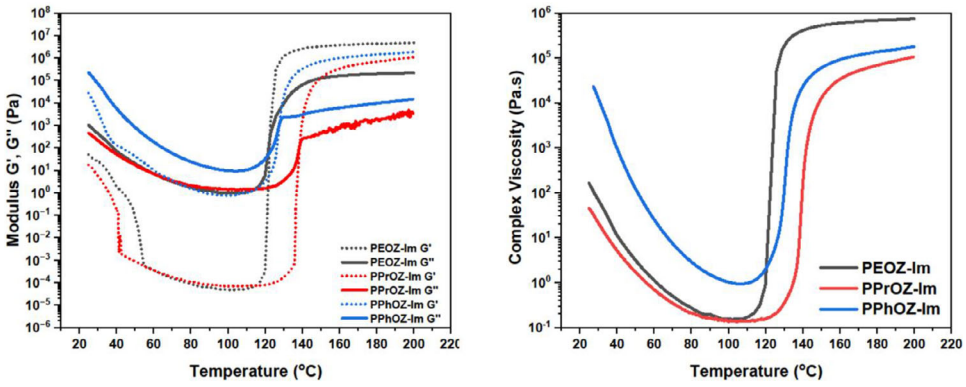

FIGURE 10 | Temperature sweep results of POZ-Im/DGEBA OCERs.

TABLE 4 | Time to reach twice the initial viscosity (min).

POZ-Im	50°C	60°C	70°C	80°C	90°C
PEOZ-Im	146	142	90	50	—
PPrOZ-Im	—	>120	108	53	36
PPhOZ-Im	—	90	48	26	18

The shelf-life values based on the rheology results at varying temperatures are provided in Table 4.

An accelerated stability study was conducted using elevated temperature (60°C, 70°C, 80°C, and 90°C) data to estimate the shelf life at low temperatures (20°C, 0°C, and −20°C) through the Arrhenius extrapolation method. The following equations are used to find the correlation between the rate constant (k) and temperature (T).

$$k = Ae^{-\frac{Ea}{RT}} \quad (1)$$

$$k = \frac{1}{t} \quad (2)$$

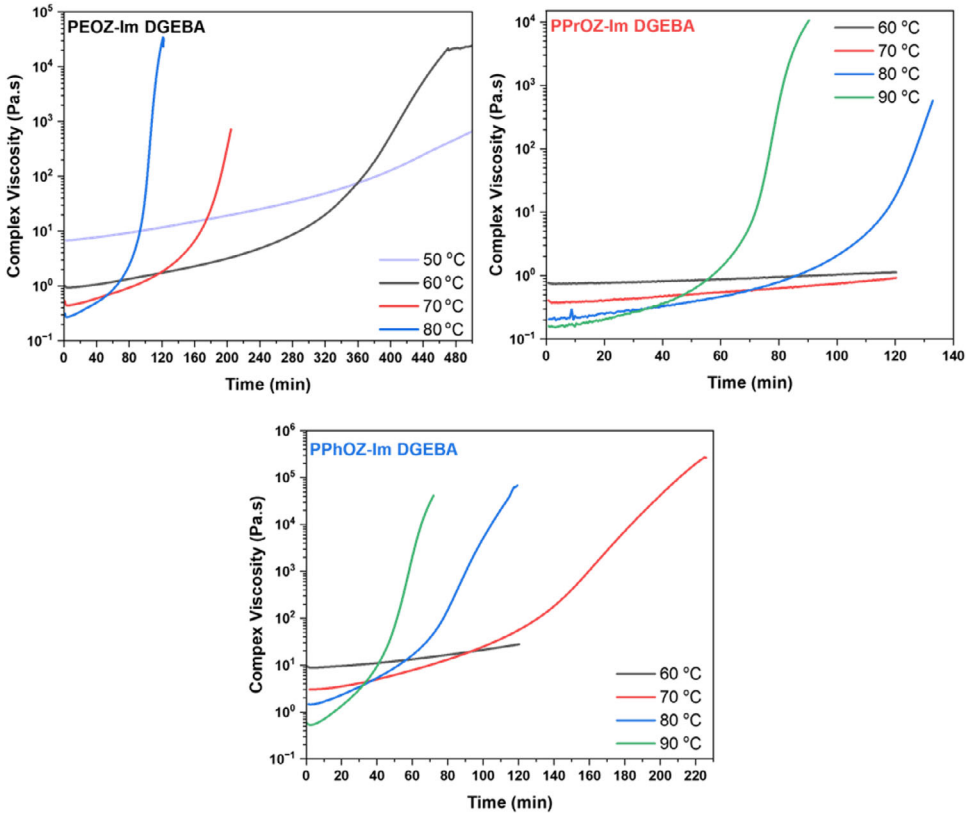

FIGURE 11 | Isothermal rheology analysis results of POZ-Im/DGEBA OCERs.

$$\ln(k) = lnA - \frac{Ea}{RT} \quad (3)$$

where k is the rate constant (1/s), A is pre-exponential factor, E_a is the activation energy (J/mol), R is the gas constant (8.314 J/molK), T is temperature (K), and t is the gel time at temperature T. By plotting ln (k) vs 1/T for each OCER formulation and fitting a linear regression, the relationship between the reaction rate constant k and temperature was found. This correlation was then used to extrapolate the rate constants and corresponding shelf lives at lower temperatures (20°C, 0°C, and −20°C). The shelf-life values and Arrhenius rate constants are summarized in Table 5 and Figure 12.

A clear linear relationship between ln(k) and 1/T is observed for all three systems, indicating that viscosity growth during storage follows an Arrhenius-type, thermally activated process. As the storage temperature decreases from 20°C to −20°C, the shelf-life of each formulation increases, demonstrating the strong influence of temperature on latency.

All three formulations show the expected increase in viscosity-doubling time as temperature decreases, confirming the thermal latency of the POZ-Im polymers. Notable differences arise among the systems. PPrOZ-Im/DGEBA OCER demonstrated the longest estimated shelf life (~2 days at 20°C, ~12 days at 0°C, and ~88 days at −20°C), while PPhOZ-Im/DGEBA OCER showed the shortest (~0.9 days at 20°C, ~5 days at 0°C, and ~32 days at −20°C). PEOZ-Im/DGEBA OCER showed intermediate stability (~1 day at 20°C, ~6 days at 0°C, and ~34 days at −20°C), closely matching the performance of PPhOZ-Im/DGEBA OCER. These differences reflect the influence of the POZ side chain structure on the thermal stability of the OCERs.

The Arrhenius rate constants further support these trends. PPrOZ-Im/DGEBA OCER shows consistently lower k values and more negative ln(k) values relative to the other systems, indicating slower viscosity increase and delayed catalytic activation. Its moderate hydrophobicity and steric hindrance are the causes of PPrOZ-Im's increased stability; the propyl side chains enhance compatibility with DGEBA while restricting imidazole mobility, thereby postponing the onset of the reaction. PEOZ-Im/DGEBA OCER, which shows high latency in DSC, displays intermediate rheological stability, with shelf-life values shorter than PPrOZ-Im/DGEBA OCER but longer than PPhOZ-Im/DGEBA OCER at every temperature. Despite its overall delay in curing as seen in DSC, PEOZ-Im's limited solubility in DGEBA leads to phase-separated domains where imidazole concentration may locally increase, which initiates premature reactivity. PPhOZ-Im/DGEBA OCER shows the shortest shelf-life across the series and the highest rate constants, indicating the lowest latency and fastest approach toward gelation once the curing reaction begins. Despite being highly miscible because of its aromatic structure, PPhOZ-Im has higher imidazole accessibility and diffusion, which is made possible by rigid packing and π–π interactions. This lowers the activation barrier and shortens shelf life. These trends align with the dynamic DSC and miscibility results: PPrOZ-Im activates the latest, PEOZ-Im activates earlier but cures moderately, and PPhOZ-Im cures most rapidly once activated.

TABLE 5 | Shelf-life data and rate constants for the POZ-Im/DGEBA OCERs based on isothermal rheology.

PEOZ-Im/DGEBA								
Temperature		**Shelf-life**				**Rate constant, lnk, and 1/T**		
T (°C)	**T(K)**	**t (s)**	**t (min)**	**t (h)**	**t (day)**	**k**	**1/T**	**Lnk**
60	333	8520	142	2.4	0.099	1.1737E-04	0.00300	−9.05017
70	343	5400	90	1.5	0.063	1.8519E-04	0.00292	−8.59415
80	353	3000	50	0.8	0.035	3.3333E-04	0.00283	−8.00637
20	293	107752	1796	29.9	**1.247**	9.2806E-06	0.00341	−11.5876
0	273	498418	8307	138.4	**5.769**	2.0063E-06	0.00366	−13.1192
−20	253	2937172	48953	815.9	**33.995**	3.4046E-07	0.00395	−14.893

PPrOZ-Im/DGEBA								
Temperature		**Shelf-life**				**Rate constant, lnk, and 1/T**		
T (°C)	**T(K)**	**t (s)**	**t (min)**	**t (h)**	**t (day)**	**k**	**1/T**	**lnk**
70	343	6480	108	1.80	0.075	1.54E-04	0.00292	−8.776
80	353	3180	53	0.88	0.037	3.14E-04	0.00283	−8.065
90	363	2160	36	0.60	0.025	4.63E-04	0.00275	−7.678
20	293	187281	3121	52.02	**2.168**	5.34E-06	0.00341	−12.140
0	273	1040020	17334	288.89	**12.037**	9.62E-07	0.00366	−13.855
−20	253	7573651	126228	2103.79	**87.658**	1.32E-07	0.00395	−15.840

PPhOZ-Im/DGEBA								
Temperature		**Shelf-life**				**Rate constant, lnk, and 1/T**		
T (°C)	**T (K)**	**t (s)**	**t (min)**	**t (h)**	**t (day)**	**k**	**1/T**	**lnk**
60	333	5400	90	1.50	0.063	1.85E-04	0.00300	−8.594
70	343	2880	48	0.80	0.033	3.47E-04	0.00292	−7.966
80	353	1560	26	0.43	0.018	6.41E-04	0.00283	−7.352
90	363	1080	18	0.30	0.013	9.26E-04	0.00275	−6.985
20	293	77677	1295	21.58	**0.899**	1.29E-05	0.00341	−11.260
0	273	403777	6730	112.16	**4.673**	2.48E-06	0.00366	−12.909
−20	253	2723754	45396	756.60	**31.525**	3.67E-07	0.00395	−14.818

Overall, the results indicate that the molecular environment and mobility of imidazole groups, in addition to miscibility, control shelf life. Physical dispersion and chemical latency both play a part in defining OCER storage stability, as evidenced by the association between longer shelf life and delayed thermal/viscosity onset.

4 | Conclusions

This work provides the first covalently bonded poly(2-oxazoline)-imidazole (POZ-Im) latent curing agents and establishes direct structure–property relationships enabling structured design of polymeric TLCs. POZ-Im polymers were developed as tunable thermal latent curing agents (TLCs) for one-component epoxy resins (OCERs) to enhance imidazole stability and improve shelf life and processability for composite applications. Homopolymers with different side chains (2-ethyl-, 2-propyl-, and 2-phenyl-) were synthesized by living cationic ring-opening polymerization and terminated directly with imidazole in a simple one-pot process. Structural analyses by ^{1}H NMR, FTIR, and MALDI-TOF confirmed well-defined end-functionalized polymers with narrow polydispersity. Thermal characterization by DSC and TGA revealed amorphous structures with high thermal stability and side-chain-dependent T_g and degradation behavior.

When incorporated into DGEBA resin with a fixed 5% imidazole-to-epoxy ratio, POZ-Im polymers exhibited distinct miscibility and latency profiles governed by their side-chain chemistry. PPhOZ-Im showed the best miscibility due to aromatic interactions with DGEBA, while PEOZ-Im formed fine dispersed domains owing to its hydrophilic nature. DSC and rheological

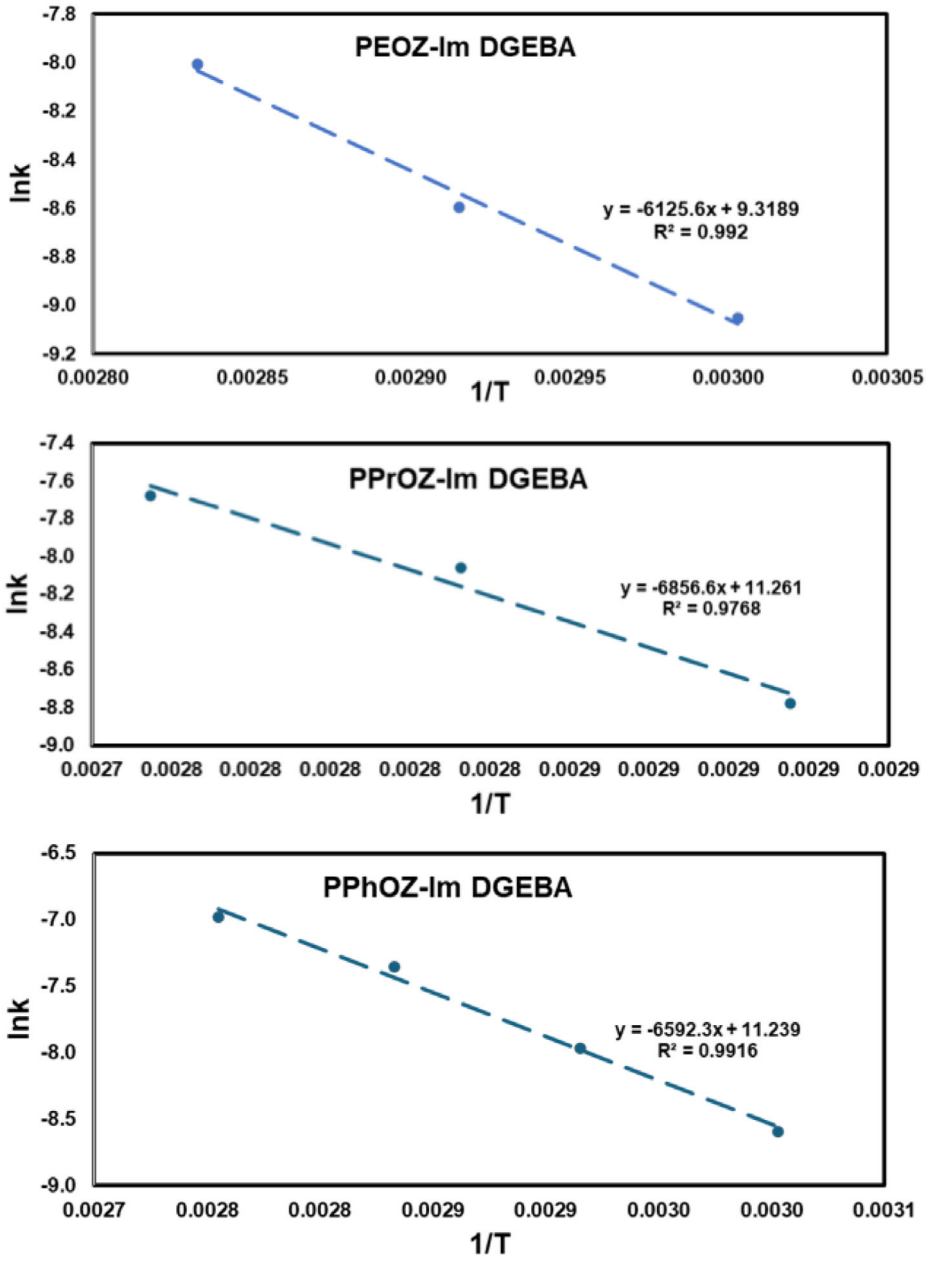

FIGURE 12 | Arrhenius plots of ln(k) vs. 1/T for the POZ-Im/DGEBA OCERs, used to extrapolate shelf lives at lower temperatures.

analyses confirmed latent curing behavior in all systems, with curing temperatures shifted higher than free imidazole. Among the three materials, PPrOZ-Im displayed the most favorable overall performance as a TLC, exhibiting the highest latency, longest gelation time, and longest shelf life. Therefore, it is the strongest candidate for OCERs and prepregs. PEOZ-Im, with moderate latency and phase-separated morphology, is suited for systems requiring balanced storage stability and earlier activation. PPhOZ-Im, which cures most rapidly once activated, is best suited for fast-curing adhesives or processing routes demanding short cycle times. It is also a promising candidate for latent accelerator roles in systems such as amine- or DICY-cured resins, an application that will be further explored in future work.

Overall, POZ-Im polymers synthesized via one-pot termination offered an easy route to well-defined polymeric TLCs with tunable curing behavior. Side-chain variation enabled precise control over miscibility, curing temperature, and latency. This study demonstrates that covalently bonded POZ-Im structures offer a straightforward and versatile platform for designing polymeric TLCs with application-specific performance, which provides promising opportunities for durable, energy-efficient, and process-stable epoxy-based composites.

Acknowledgements

The authors would like to thank Sabanci University Integrated Manufacturing Technologies Research and Application Center (SU-IMC) for providing laboratory facilities and technical support.

Funding

This work was supported by the Scientific and Technological Research Council of Turkey (TUBITAK) with project code 121Z597.

Conflicts of Interest

The authors declare no conflicts of interest.

Data Availability Statement

The data that support the findings of this study are available from the corresponding author upon reasonable request.

References

1. S. Sajan and D. Philip Selvaraj, "A Review on Polymer Matrix Composite Materials and Their Applications," *Materials Today: Proceedings* 47 (2021): 5493–5498, https://doi.org/10.1016/j.matpr.2021.08.034.

2. R. Hsissou, R. Seghiri, Z. Benzekri, M. Hilali, M. Rafik, and A. Elharfi, "Polymer Composite Materials: A Comprehensive Review," *Composite Structures* 262 (2021): 113640, https://doi.org/10.1016/j.compstruct.2021.113640.

3. F.-L. Jin, X. Li, and S.-J. Park, "Synthesis and Application of Epoxy Resins: A Review," *Journal of Industrial and Engineering Chemistry* 29 (2015): 1–11, https://doi.org/10.1016/j.jiec.2015.03.026.

4. C. Acebo, X. Ramis, and A. Serra, "Improved Epoxy Thermosets by the Use of Poly(ethyleneimine) Derivatives," *Physical Sciences Reviews* 2, no. 8 (2017): 20160128, https://doi.org/10.1515/psr-2016-0128.

5. P. Mohan, "A Critical Review: The Modification, Properties, and Applications of Epoxy Resins," *Polymer-Plastics Technology and Engineering* 52, no. 2 (2013): 107–125, https://doi.org/10.1080/03602559.2012.727057.

6. K. Zhang, Z. Wang, and Y. Luo, "One-Component Epoxy Resin Adhesive Featured with High Storage Stability Based on Microencapsulation," *Colloids and Surfaces A: Physicochemical and Engineering Aspects* 683 (2024): 133045, https://doi.org/10.1016/j.colsurfa.2023.133045.

7. Q. Zhang, J. Wang, S. Yang, J. Cheng, G. Ding, and S. Huo, "Facile Construction of One-Component Intrinsic Flame-Retardant Epoxy Resin System with Fast Curing Ability Using Imidazole-Blocked Bismaleimide," *Composites Part B: Engineering* 177 (2019): 107380, https://doi.org/10.1016/j.compositesb.2019.107380.

8. Y. R. Ham, D. H. Lee, S. H. Kim, Y. J. Shin, M. Yang, and J. S. Shin, "Microencapsulation of Imidazole Curing Agent for Epoxy Resin," *Journal of Industrial and Engineering Chemistry* 16, no. 5 (2010): 728–733, https://doi.org/10.1016/j.jiec.2010.07.011.

9. P. Zhang, S. A. Ali Shah, and F. Gao, "Latent Curing Epoxy Systems with Reduced Curing Temperature and Improved Stability," *Thermochimica Acta* 676 (2019): 130–138, https://doi.org/10.1016/j.tca.2019.03.022.

10. Y. Ito, D. Aoki, and K. Arimitsu, "Novel Thermal Latent Curing Agents for Epoxy Resins Based on Dual-Locked Aminopyridines by Amidation and *N* -Oxidation," *Macromolecules* 58, no. 6 (2025): 2870–2878, https://doi.org/10.1021/acs.macromol.4c02707.

11. W.-P. Yen, K.-L. Chen, M.-Y. Yeh, N. Uramaru, H.-Y. Lin, and F. F. Wong, "Investigation of Soluble PEG-Imidazoles as the Thermal Latency Catalysts for Epoxy-Phenolic Resins," *Journal of the Taiwan Institute of Chemical Engineers* 59 (2016): 98–105, https://doi.org/10.1016/j.jtice.2015.08.007.

12. K.-L. Chen, Y.-H. Shen, M.-Y. Yeh, and F. F. Wong, "Complexes of Imidazole with Poly(ethylene glycol)s as the Thermal Latency Catalysts for Epoxy–Phenolic Resins," *Journal of the Taiwan Institute of Chemical Engineers* 43, no. 2 (2012): 306–312, https://doi.org/10.1016/j.jtice.2011.08.007.

13. M. Fuensanta, A. Grau, M. D. Romero-Sánchez, C. Guillem, and Á. M. López-Buendía, "Effect of the Polymer Shell in Imidazole Microencapsulation by Solvent Evaporation Method," *Polymer Bulletin* 70, no. 11 (2013): 3055–3074, https://doi.org/10.1007/s00289-013-1007-z.

14. M. J. Shin, Y. J. Shin, and J. S. Shin, "Latent Imidazole Curing Agents by Microencapsulation with Copolymers," *Particulate Science and Technology* 36, no. 1 (2018): 112–116, https://doi.org/10.1080/02726351.2016.1226224.

15. S. Xing, J. Yang, Y. Huang, Q. Zheng, and J. Zeng, "Preparation and Characterization of a Novel Microcapsule-Type Latent Curing Agent for Epoxy Resin," *Materials & Design* 85 (2015): 661–670, https://doi.org/10.1016/j.matdes.2015.07.098.

16. A. E. Atespare, T. Behroozi Kohlan, and S. Salamatgharamaleki, "Poly(2-alkyl/aryl-2-oxazoline)-Imidazole Complexes as Thermal Latent Curing Agents for Epoxy Resins," *ACS Omega* 9 (2024): 36398–36410, https://doi.org/10.1021/acsomega.4c03904.

17. T. B. Kohlan, A. E. Atespare, M. Yildiz, Y. Z. Menceloglu, S. Unal, and B. Dizman, "Amphiphilic Polyoxazoline Copolymer–Imidazole Complexes as Tailorable Thermal Latent Curing Agents for One-Component Epoxy Resins," *ACS Omega* 8, no. 49 (2023): 47173–47186, https://doi.org/10.1021/acsomega.3c07177.

18. B. Dizman, S. Unal, Y. Z. Menceloglu, M. Yildiz, T. B. Kohlan, and A. E. Atespare, Polyoxazoline Based Thermal Latent Curing Agents for Thermoset Resins. European Patent EP4430102B1, June 25, 2025.

19. C.-C. Tseng, K.-L. Chen, K.-W. Lee, H. Takayam, C.-Y. Lin, and F. F. Wong, "Soluble PEG600-Imidazole Derivatives as the Thermal Latent Catalysts for Epoxy-Phenolic Resins," *Progress in Organic Coatings* 127 (2019): 385–393, https://doi.org/10.1016/j.porgcoat.2018.12.003.

20. P. Reuther, P. Dünnwald, M. Tabatabai, C. Schuh, L. Hartmann, and H. Ritter, "Thermally Controlled Acceleration of Epoxy Resin Curing through Polymer-Bound Imidazole Derivatives with High Latency," *ACS Applied Polymer Materials* 4, no. 2 (2022): 1150–1158, https://doi.org/10.1021/acsapm.1c01568.

21. T. X. Viegas, Z. Fang, K. Yoon, R. Weimer, and B. Dizman, "Poly(oxazolines)," *Engineering of Biomaterials for Drug Delivery Systems* (Woodhead Publishing, 2018): 173–198, https://doi.org/10.1016/B978-0-08-101750-0.00006-425.

22. T. X. Viegas, M. D. Bentley, and J. M. Harris, "Polyoxazoline: Chemistry, Properties, and Applications in Drug Delivery," *Bioconjugate Chemistry* 22, no. 5 (2011): 976–986, https://doi.org/10.1021/bc200049d.

23. A. E. Atespare, T. B. Kohlan, and S. Salamatgharamaleki, "Structure–Property Relationship and Epoxy Resin Compatibility of Poly(2-alkyl/aryl-2-oxazoline)s, alongside Rheological Properties of Their Blends," *Polymer Engineering & Science* 65 (2025): 3193–3208, https://doi.org/10.1002/pen.27208.

24. R. W. Moreadith, T. X. Viegas, and M. D. Bentley, "Clinical development of a poly(2-Oxazoline) (POZ) polymer therapeutic for the treatment of Parkinson's Disease – Proof of concept of POZ as a versatile polymer platform for drug development in multiple therapeutic indications," *European Polymer Journal* 88 (2017): 524–552, https://doi.org/10.1016/j.eurpolymj.2016.09.052.

25. R. Hoogenboom and H. Schlaad, "Bioinspired Poly(2-Oxazoline)s," *Polymers* 3, no. 1 (2011): 467–488, https://doi.org/10.3390/polym3010467.

26. R. Hoogenboom and H. Schlaad, "Thermoresponsive Poly(2-Oxazoline)s, Polypeptoids, and Polypeptides," *Polymer Chemistry* 8, no. 1 (2017): 24–40, https://doi.org/10.1039/C6PY01320A.

27. T. B. Kohlan, A. E. Atespare, M. Yildiz, Y. Z. Menceloglu, S. Unal, and B. Dizman, "Synthesis and Structure–Property Relationship of Amphiphilic Poly(2-ethyl-co-2-(alkyl/aryl)-2-oxazoline) Copolymers," *ACS Omega* 7, no. 44 (2022): 40067–40077, https://doi.org/10.1021/acsomega.2c04809.

28. E. F.-J. Rettler, J. M. Kranenburg, H. M. L. Lambermont-Thijs, R. Hoogenboom, and U. S. Schubert, "Thermal, Mechanical, and Surface Properties of Poly(2- N -alkyl-2-oxazoline)s," *Macromolecular Chemistry*

and Physics 211, no. 22 (2010): 2443–2448, https://doi.org/10.1002/macp.201000338.

29. K. Kempe, M. Lobert, R. Hoogenboom, and U. S. Schubert, "Screening the Synthesis of 2-Substituted-2-oxazolines," *Journal of Combinatorial Chemistry* 11, no. 2 (2009): 274–280, https://doi.org/10.1021/cc800174d.